

RESEARCH ARTICLE

Women's Health Research and Novel Perspectives on Sex as an Investigative Variable

Sex chromosomes and gonadal sex interactions in airway and immune responses to allergen challenge

 Carolyn Damilola Ekpruke,¹  Dustin Roussele,¹ Rachel Alford,¹  Omar Borges-Sosa,¹
 Maksat Babayev,¹  Shikha Sharma,¹ Lydia Dinwiddie,¹ Erik Parker,² Sarah Bradley,¹
Matthew Louis Retzner,¹ and  Patricia Silveyra^{1,3}

¹Department of Environmental and Occupational Health, School of Public Health, Indiana University, Bloomington, Indiana, United States; ²Biostatistics Consulting Center, Department of Epidemiology and Biostatistics, School of Public Health, Indiana University, Bloomington, Indiana, United States; and ³School of Medicine, Indiana University, Indianapolis, Indiana, United States

Abstract

Asthma is a chronic respiratory condition influenced by genetic, environmental, and sex-related factors. Women experience greater asthma severity, airway hyperresponsiveness (AHR), and inflammation than men, likely due to sex-linked genetic and hormonal differences. However, the independent contributions of sex chromosomes and gonadal sex to these responses remain unclear. This study examines their roles in allergic airway responses using the four core genotype (FCG) mouse model, which distinguishes between chromosomal and gonadal influences. We hypothesized that XX-mice and those with female gonads would exhibit heightened airway inflammation and immune activation in response to house dust mite (HDM) challenge. Using a controlled, moderate 5-wk HDM exposure paradigm that reliably induced allergic airway inflammation, we aimed to capture biologically relevant sex- and genotype-dependent variations rather than a maximal inflammatory phenotype. FCG mice (XXF, XXM, XYF, and XYM) underwent 5 wk of HDM exposure, followed by assessments of airway lung function and inflammation. Our results showed that HDM challenge differentially increased airway resistance and elastance in FCG mice, with specific contributions of sex chromosomes and gonadal sex. Histological analysis showed higher lung inflammation and goblet cell hyperplasia in challenged mice with female gonads than in those with male gonads. Flow cytometry assessment revealed elevated eosinophils in XXF mice. Combined, our findings show that both sex chromosomes and gonadal sex influence airway inflammation and immune responses to allergen challenge, with mice bearing XX chromosomes and female gonads exhibiting greater susceptibility.

NEW & NOTEWORTHY This study provides new insights into how sex chromosomes and gonadal sex independently and interactively shape immune cell responses during allergic airway inflammation. Using the four core genotype (FCG) mouse model, we show that both genetic and hormonal factors significantly influence pulmonary immune cell populations after allergen exposure. These findings advance our understanding of the biological basis for sex differences in asthma and highlight the need for sex-informed approaches in respiratory disease research and therapy development.

allergic airway inflammation; four core genotype (FCG) model; gonadal hormones; immune cell profiling; sex chromosomes

INTRODUCTION

Asthma is a chronic respiratory condition characterized by airway inflammation, remodeling, and hyperresponsiveness (1). Asthma affects over 262 million individuals globally and 25 million in the United States, contributing to approximately 455,000 deaths annually (2, 3). Genetic, occupational, and environmental factors contribute to asthma, which manifests with varying degrees of inflammation depending on disease severity (4). Previous studies have established that inflammatory changes are distinctly seen in the airways of asthmatics

(5) and are positively correlated with disease severity (6). The complexity of asthma is further compounded by observed sex disparities in symptom severity, contributing to challenges in developing effective therapeutics. Although significant progress has been made in understanding allergic airway inflammation and its link to asthma phenotypes in males and females, no sex-specific treatments have been developed to date.

An association between house dust mites (HDMs), a common aeroallergen, and asthma has been reported in approximately 85% of individuals worldwide, particularly



Correspondence: P. Silveyra (psilveyr@iu.edu).

Submitted 20 June 2025 / Revised 21 July 2025 / Accepted 16 January 2026



in developed countries (7, 8). The predominant HDM species are *Dermatophagoides pteronyssinus* and *D. farina* (9). HDM fecal particles can penetrate the respiratory epithelium, inducing inflammation and bronchoconstriction (10, 11). Animal models of HDM-induced allergic airway inflammation have provided valuable insights into asthma pathogenesis (12, 13), closely recapitulating human disease features such as eosinophilic infiltration, airway hyperresponsiveness, and goblet cell hyperplasia (14).

The roles of sex hormones and sex chromosomes in respiratory disease are critical yet underexplored areas of research (15). Males possess a sex chromosome complement of XY, whereas females have XX. During development, the presence of the SRY gene on the Y chromosome initiates testis formation, while its absence results in ovary development. The four core genotype (FCG) mouse model is particularly suited to dissect the independent effects of sex chromosomes and gonadal sex on allergic airway inflammation (16). This model includes four genotypes, XXM, XXF, XYM, and XYF, allowing the effects of chromosomal complement (XX vs. XY) and gonadal type (male vs. female) to be evaluated separately.

Innate and adaptive immune responses differ between males and females, influencing allergic airway inflammation. Females generally exhibit stronger humoral and cell-mediated immune responses than males (17–22). Sex hormones contribute significantly to these differences: testosterone suppresses proinflammatory cytokine expression and natural killer (NK) cell activity while promoting anti-inflammatory IL-10 expression (23–26), whereas estradiol modulates both innate and adaptive immunity in a concentration-dependent manner, enhancing Th2 responses and regulatory T-cell expansion at higher levels (27–31). Progesterone also promotes Th2-skewed immunity and regulatory T cell proliferation while suppressing Th1 responses (32, 33). These hormonal effects collectively influence the inflammatory and remodeling processes characteristic of asthma (34).

Sex chromosomes complement further modulate immune regulation relevant to allergic airway disease. Several immune-related genes located on the X chromosome, including *Foxp3*, exhibit differential expression between sexes and may contribute to sex-specific susceptibility to airway inflammation (35–38). Polymorphisms and regulatory variants on the Y chromosome have also been linked to male-specific immune modulation (39–41). Thus, both hormonal and chromosomal factors act in concert to shape immune responses and airway remodeling.

Collectively, sex steroids and sex chromosome complement modulate immune cell activity, airway inflammation, and remodeling, highlighting their relevance in asthma and allergic airway disease. However, the distinct contributions of sex chromosomes and gonadal hormones to allergic airway inflammation remain poorly understood. Previous research from our laboratory (42) and others (43) has demonstrated sex-specific airway responses to HDM exposure, with females showing greater lung inflammatory gene expression compared with males. The current study expands on these findings to examine how sex chromosomes and gonadal sex interact to influence airway inflammation, immune cell infiltration, and airway hyperresponsiveness (AHR). Using the FCG model, we used a moderate, chronic HDM exposure protocol to induce reproducible allergic airway inflammation

while maintaining sensitivity to sex- and genotype-dependent effects rather than eliciting maximal inflammation.

MATERIALS AND METHODS

Animals

The protocol for this animal study was approved by the Bloomington Institutional Animal Care and Use Committee (BIACUC) at Indiana University before the start of the study (Protocols 21-012 and 24-020). The study was conducted following the National Institutes of Health (NIH) guidelines for the care and use of laboratory animals. Female wild-type mice and XYM mice of C57BL/6J background were purchased from The Jackson Laboratory (Bar Harbor, ME, USA; stock no. 010905) and bred in-house following the approved protocol. The resulting offspring represent the four core genotype mice model (XYM, XYF, XXM, and XXF). Genomic PCR was performed at 4–5 wk of age to confirm the genotype of each animal following the protocol provided by The Jackson Laboratory. Mice were grouped according to their genotypes and used in the study at 8–10 wk of age ($n = 3–11$ mice per group).

Intranasal Instillation of Allergen Challenge

The control group received 50 μ L of phosphate-buffered saline (PBS) intranasally, while the experimental group was challenged with 50 μ L of HDM solution containing 25 μ g of HDM extract from *D. pteronyssinus* and *D. farina*, 5 days/week for 5 wk. The HDM solution was prepared by resuspending 25 μ g of HDM extract (Citeq Biologics, Groningen, The Netherlands) in 25 μ L PBS. Both PBS and HDM were administered intranasally to FCG mice using 20–200 μ L pipette tips after light anesthesia with 5% isoflurane. This 5-wk dosing regimen produces a moderate, sustained airway inflammation phenotype characterized by measurable AHR and immune infiltration, consistent with previous HDM studies in C57BL/6 mice (13, 14). At 72 h after the last exposure, airway hyperresponsiveness (AHR) was assessed through Methacholine (MCh) challenge, and lungs were harvested for flow cytometry and histological analysis in all the mice as described below.

Airway Hyperresponsiveness through MCh Challenge

Animals were anesthetized with an intraperitoneal injection of ketamine (100 mg/kg) and xylazine (10 mg/kg), after which a tracheostomy was performed using an 18-gauge cannula. The mice were then connected to a rodent ventilator (flexiVent, SCIREQ, Montreal, Canada). Pancuronium bromide (10 mg/kg) was administered to induce muscle paralysis. Ventilation settings included a positive end-expiratory pressure (PEEP) of 3 cmH₂O, a tidal volume of 10 mL/kg, and a maximum inflation pressure of 30 cmH₂O. After establishing baseline measurements, MCh was administered by nebulization at concentrations of 0, 3.13, 12.5, 25, 50, and 100 mg/mL. The peak response was measured using six perturbations at each dose of MCh. Total airway Resistance (Rrs) and elastance (Ers) indicate lung stiffness; conducting airway resistance (Rn) reflects central airway caliber and bronchoconstriction, whereas tissue resistance (G) and tissue elastance (H) reflect peripheral tissue mechanics and

heterogeneity of parenchymal impedance. Changes in these parameters, which collectively indicate airway narrowing and parenchymal involvement relevant to asthma pathophysiology, were recorded before and after each MCh dose.

Histological Assessment

Animals were anesthetized with ketamine (100 mg/kg) and xylazine (10 mg/kg) and exsanguinated. The chest cavity was opened, the trachea cannulated, and 5 mL of formalin was administered through a syringe located at a vertical height of 25 cm from the animal, allowing the lungs to be perfused by gravity. The lungs were then fixed in formalin overnight. After 24 h, the lungs were transferred to a 70% ethanol solution. Each lung lobe was halved, sectioned, and stained with hematoxylin & eosin or Alcian Blue & Periodic Acid Schiff at the Indiana University School of Medicine Histology Core, following a published method (44). Three blinded investigators examined all tissue samples for perivascular inflammation, peribronchial inflammation, and goblet cell hyperplasia by microscopy. A semiquantitative scoring system was used, with inflammation and epithelial changes graded on a scale from 0 to 4, where 0 indicated no inflammation or hyperplasia, and 4 indicated severe infiltration or extensive goblet cell proliferation. Scores were assigned based on inflammatory cell cuffing, the extent of alveolar infiltration, and the degree of epithelial remodeling. For each animal, multiple nonoverlapping fields at 20x magnification were analyzed, and mean scores for each parameter were calculated for further statistical analysis.

Quantification of PAS-positive cells.

To further assess epithelial remodeling, Alcian Blue-Periodic Acid-Schiff (AB-PAS) stained lung sections were analyzed using QuPath (v. 0.4.3) for quantitative evaluation of PAS-positive epithelial cells. For each mouse, airway regions were annotated manually at $\times 20$ magnification. PAS-positive goblet cells were detected using a color deconvolution and thresholding algorithm, verified manually, and expressed as the number of PAS-positive cells normalized to the area of basement membrane in mm^2 of airways per section (cells/mm^2). Data from animals in the same group and treatment were statistically analyzed.

Isolation of immune cells and flow cytometry analysis.

Mice from each group were anesthetized with ketamine (100 mg/kg) and xylazine (10 mg/kg). The lungs were perfused by flushing with 10 mL of cold PBS using a 10-mL syringe and a 25-G needle. Lung tissue was then placed in a c-tube containing 2.4 mL of Buffer S, 15 μL of Enzyme A, and 100 μL of Enzyme D (Miltenyi Biotec, #130-095-927) and homogenized using the gentleMACS dissociator (Miltenyi Biotec, #130-093-235). The homogenized tissue was incubated at 37°C for 30 min, followed by a second homogenization on the dissociator. The solution was filtered through sterile SmartStrainers (70 μm , Miltenyi Biotec) and rinsed with 2.5 mL of buffer S in a 15-mL tube. Cells were then washed twice with PEB buffer (Miltenyi Biotec), pelleted, and resuspended in 500 μL PEB buffer. Lung tissue, rather than bronchoalveolar lavage (BAL), was selected to capture

both airway wall and interstitial immune populations often underrepresented in lavage samples.

For analysis, cells were divided into separate tubes and stained with antibodies according to cell type. Antibodies were organized into three sets to identify 13 different cell types, as shown in previous studies (45, 46). Samples were incubated with antibodies at room temperature for 30 min, washed with PEB buffer, and resuspended in 300 μL of PEB buffer for flow cytometry analysis using a Beckman Coulter Life Sciences 4-laser (V-B-Y-R) CytoFLEX LX by the flow cytometry core facility (Bloomington, IN). For each lung tissue sample, $\sim 1 \times 10^6$ viable cells were obtained following enzymatic dissociation. Data acquisition was performed on a Beckman Coulter CytoFLEX LX cytometer, with 100,000 total events collected per sample. For fluorescence minus one (FMO), compensation, and unstained negative controls, 50,000 events were collected to ensure accurate gating and fluorophore compensation. The antibody panels, staining validation, and gating strategy used here have been previously published (46) and are consistent with our prior methods. Zombie NIR (Fixable viability dye) was used to distinguish live and dead cells. Data were then analyzed with FlowJo software (FlowJo LLC, Oregon).

The cells identified with *Set 1* of antibodies included alveolar macrophages (AMs), eosinophils, CD103^+ dendritic cells (DCs), CD11b^+ DCs, and interstitial macrophages. *Set 2* antibodies identified undifferentiated monocytes and neutrophils, whereas *Set 3* antibodies identified plasmacytoid DCs, B cells, CD4^+ T-cells, CD8^+ T-cells, NK cells, and NKT cells (46).

Flow cytometry gating and validation strategy. The gating strategy for this study was adapted from a previously published approach (45) and refined using established methods from our laboratory (46). Surface markers for immune-cell identification are listed in our prior publication (46), and all gating was performed on live cell populations. Unstained cells and fluorescence-minus-one (FMO) controls were included in every experiment to define positive and negative boundaries among immune-cell subsets, while single-color controls ensured accurate fluorophore compensation. FMO and unstained controls were run for each experimental set (*Sets 1, 2, and 3*; Supplemental Figs. S1 and S2).

Gating boundaries for eosinophils and alveolar macrophages (AMs) were defined using FMO controls rather than fixed fluorescence-intensity thresholds to account for known biological variability in Siglec-F expression between naïve (PBS-treated) and inflamed (HDM-treated) conditions (Supplemental Fig. S2). This adjustment ensured accurate identification of eosinophils and AMs across all treatment groups. FMO controls were also used for each fluorochrome to correct for spectral overlap. The sources, dilutions, and validation of all antibodies used in this study have been described previously (46) and are summarized in Table 1. The full gating scheme and antibody-validation procedures are detailed in our earlier publication (46).

Supplemental Figs. S1–S6 collectively illustrate the validation workflow, gating hierarchy, and representative plots used to identify immune-cell subsets from enzymatically dissociated whole-lung tissue of four core genotype (FCG) mice following PBS or HDM exposure. The gating workflow began with the exclusion of debris and doublets, followed by selection of live CD45^+ Zombie NIR⁻ leukocytes and sequential

Table 1. Flow cytometry antibodies and staining reagents

Catalog No.	Target	Fluorochrome	Quantity	Company Name
103212	B220 /CD45R	APC	0.25 µg per 10 ⁶ cells in 100 µL volume	BioLegend
150605	CCR2	BV421	0.5 µg per million cells in 100 µL volume	BioLegend
121422	CD103	BV421	5 µL per million cells in 100 µL staining volume	BioLegend
101216	CD11b	PE/Cy7	0.25 µg per 10 ⁶ cells in 100 µL volume	BioLegend
117318	CD11c	PE/Cy7	0.25 µg per 10 ⁶ cells in 100 µL volume	BioLegend
117328	CD11c	PerCP/Cyanine5.5	1.0 µg per million cells in 100 µL volume	BioLegend
100438	CD4	BV421	5 µL per million cells in 100 µL	BioLegend
103108	CD45	FITC	0.25 µg per 10 ⁶ cells in 100 µL volume	BioLegend
139306	CD64	APC	1.0 µg per million cells in 100 µL volume	BioLegend
100708	CD8	PE	0.25 µg per 10 ⁶ cells in 100 µL volume	BioLegend
128008	Ly6c	PE	0.25 µg per 10 ⁶ cells in 100 µL	BioLegend
127633	Ly6g	BV510	0.5 µg per million cells in 100 µL volume	BioLegend
107635	MHCII	BV510	5 µL per million cells in 100 µL staining volume	BioLegend
108728	Nk1.1	PerCP/Cyanine5.5	1.0 µg per million cells in 100 µL volume	BioLegend
155506	Siglec F	PE	0.25 µg per million cells in 100 µL volume	BioLegend
109234	TCRb	BV510	5 µL per million cells in 100 µL staining volume	BioLegend
423106	Dead cell stain	Zombie NIR	1:100 for 1–10 million cells	BioLegend
156604	TruStain FcX (anti-mouse CD16/32) Antibody	N/A	1.0 µg per 10 ⁶ cells in 100 µL volume	BioLegend

Catalog number, target antigen, conjugated fluorochrome, quantity per staining (reported per 10⁶ cells in 100 µL staining volume unless otherwise noted), and vendor are shown.

identification of major immune-cell populations, including alveolar macrophages, eosinophils, dendritic-cell subsets (CD11b⁺ and CD103⁺ DCs), plasmacytoid DCs, interstitial macrophages, T and B lymphocytes, natural killer (NK) and natural killer T (NKT) cells, as well as myeloid populations such as monocytes and neutrophils. DCs subsets were defined using MHC II expression in combination with CD103 or CD11b markers (i.e., MHCII⁺CD103⁺ DCs and MHCII⁺CD11b⁺ DCs), and interstitial macrophages were identified as MHCII⁺CD64⁺ cells, as shown in Supplemental Figs. S2 and S5. FMO and unstained controls were used to set positive and negative gates and adjust for fluorochrome spillover.

Gates were modified per sample to accommodate biological variation in marker intensity, particularly the downregulation of Siglec-F on AMs during HDM-induced inflammation, ensuring consistent discrimination of all immune populations across genotypes and treatments. These validation plots (Supplemental Figs. S1–S6) confirm that the gating and antibody-staining strategies were reproducible, accurate, and aligned with current best-practice standards for flow-cytometry rigor and reproducibility.

Statistical analysis. All statistical analyses were conducted in R version 4.3.0, using the emmeans (47), ggpubr (48), gtsummary (49), lmerTest (50), and tidyverse packages (51) by the Indiana University Biostatistics Consulting Center. To evaluate the relationships between treatment (PBS or HDM) and their interactions with sex chromosome composition (XX or XY), gonadal sex (M or F), or genotype (XXF, XXM, XYF, XYM) for each outcome, both linear and linear mixed models were employed. Separate regression models were applied to analyze data from AHR, histology, and flow cytometry datasets. Mean values for each parameter were calculated, and graphical representations were generated to illustrate group differences using GraphPad Prism v. 10.5.2.

For the AHR (flexiVent) data set, which included repeated measurements across five MCh doses (0 to 100 mg/mL) per animal, linear mixed models with random intercepts per animal were used to account for within-animal correlations. These models incorporated the main effects for dose, a

three-way interaction term between dose, treatment, and each sex variable (modeled separately), along with all relevant two-way interaction terms.

For the histology and flow cytometry datasets, where each measurement was obtained once per animal, standard linear regression models were used to assess outcomes. In all models, Type III sum of squares was applied to determine the statistical significance of main effects and interactions. When significant interaction terms were detected, pairwise estimated marginal means (EMMs) were calculated to compare outcome estimates across dose, treatment, and sex variables as appropriate.

To account for multiple comparisons, pairwise comparisons involving three or more groups were adjusted using Tukey's method, controlling for Type I family-wide error rate (FWER). Model assumptions, including normality of residuals and homoscedasticity, were assessed visually, and multicollinearity was determined to be low.

RESULTS

Airway Hyperresponsiveness

Airway hyperresponsiveness, assessed through the MCh challenge in mice from the FCG (XYM, XXM, XYF, and XXF), showed a dose-dependent effect to MCh on all lung function parameters measured (Rrs, Ers, Rn, G, and H) (Supplemental Figs. S7–S11).

The respiratory system resistance (Rrs) showed significant independent effects for MCh, treatment type (HDM or PBS), and genotype ($P < 0.001$, 0.027, and 0.046, respectively). In addition, significant interactions were noted between genotype and MCh doses ($P < 0.001$) and between gonadal sex and MCh doses ($P = 0.005$). The highest Rrs values occurred at the 100 mg/mL dose across all HDM-treated groups. Among HDM-treated mice, the XXM genotype exhibited the highest mean Rrs (1.737 ± 0.239 cmH₂O·s/mL), while the XYM genotype had the lowest (1.105 ± 0.118 cmH₂O·s/mL), though this difference was not statistically significant. In the XXF

genotype, the Rrs was significantly elevated at 100 mg/mL MCh doses compared with PBS-treated XXF mice receiving the same doses ($P = 0.039$, Supplemental Fig. S7A). When analyzing the effects of sex chromosomes independent of gonadal sex, HDM-treated XX-mice had significantly higher Rrs values compared with XY-mice at 100 mg/mL MCh ($P = 0.017$). Similarly, HDM-treated mice with female gonadal sex showed significantly higher Rrs compared with female PBS-treated mice at the same MCh dose ($P = 0.014$). Independent effect of MCh dose remained significant for the three models, sex chromosomes, gonads, and genotypes ($P < 0.001$ for all comparisons; Supplemental Fig. S7, A–D). Also, the two-way interactions between sex chromosomes and dose, gonadal sex and dose, and genotypes and dose were significant ($P = 0.001$, 0.005 , and <0.001 , respectively).

The elastance of the lungs (Ers) was also higher at the 100 mg/mL MCh dose across all groups (Fig. 1A). In the model evaluating the effects of treatment, gonadal sex, and dose, including their three-way interaction and all corresponding two-way interactions, the independent effects of treatment ($P = 0.031$) and dose ($P < 0.001$) were statistically significant. In addition, significant two-way interactions were observed between treatment and dose ($P = 0.001$), as well as gonadal sex and dose ($P = 0.043$). In the model incorporating treatment, genotype, and dose, the three-way interaction among these variables was also statistically significant

($P = 0.006$). Significant two-way interactions were found between genotype and dose, and between treatment and dose ($P = 0.001$ for both comparisons). The independent effects of treatment ($P = 0.032$) and dose ($P < 0.001$) remained significant in this model. Finally, the model including treatment, sex chromosome complement, and dose revealed significant independent effects of treatment and dose ($P = 0.026$, <0.001 , respectively) and two-way interactions between treatment and dose ($P = 0.001$) and between sex chromosomes and dose ($P = 0.005$). The Ers was higher in all HDM-treated groups compared with PBS-treated counterparts, though the increase was relatively modest (Supplemental Fig. S8, A–D). Among HDM-treated groups at 100 mg/mL MCh, the XXM exhibited the highest Ers value (53.466 ± 10.179 cmH₂O·s/mL), while the XYM mice had the lowest (30.308 ± 2.538 cmH₂O·s/mL). In XXM mice, the Ers was significantly elevated at the 100 mg/mL MCh dose in HDM-treated animals compared with their PBS-treated counterparts ($P < 0.0001$; Supplemental Fig. S8B). Within the HDM-treated FCG mice, animals with the XXM genotype had significantly higher Ers values at the 100 mg/mL dose than those with XYF ($P = 0.001$) and XYM ($P < 0.0001$) genotypes. When combined, HDM-challenged XX-mice had significantly higher Ers at the 100 mg/mL MCh dose than the control, irrespective of gonadal sex ($P < 0.0001$) and the HDM-treated XY-mice ($P < 0.0001$) (Fig. 1B). Similarly, HDM-treated mice

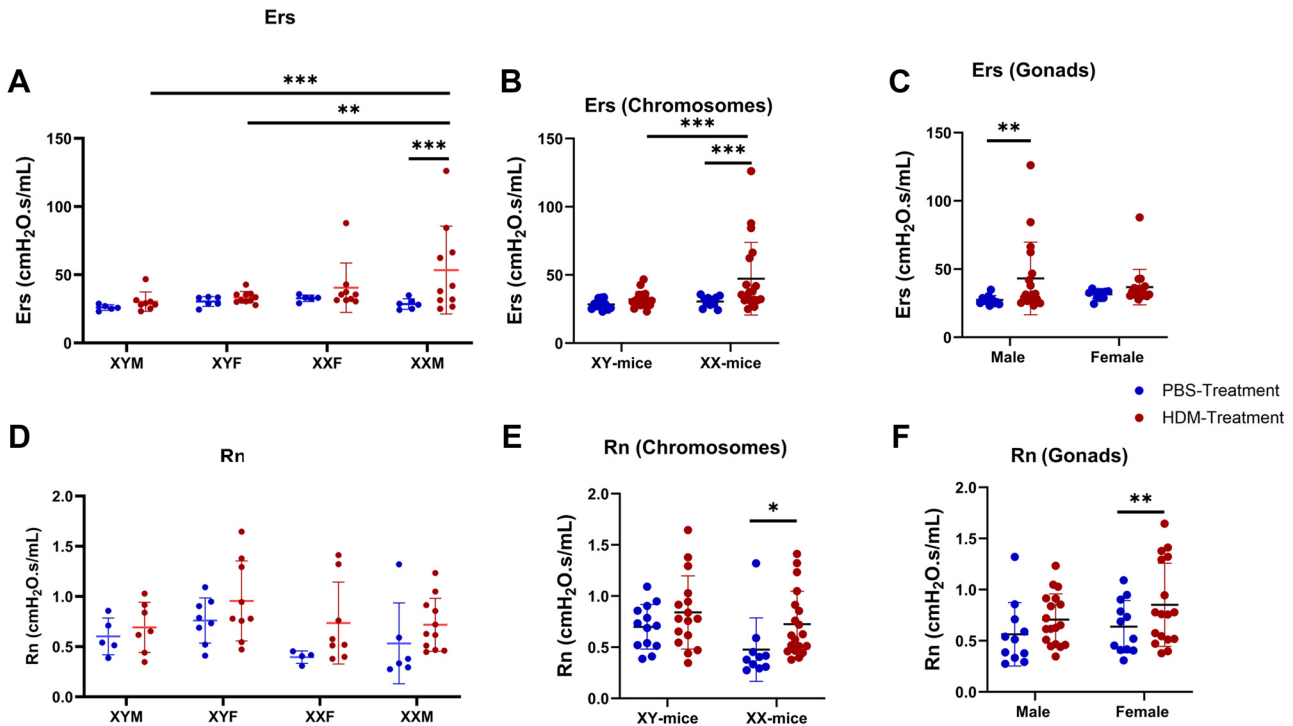


Figure 1. Airway hyperresponsiveness in the FCG mice following 5 wk HDM or PBS exposure. Assessing the influence of sex chromosome and gonadal sex in airway hyperresponsiveness using the lung parameters, Elastance (Ers) and conducting airway resistance (Rn) in the FCG mice after Methacholine (100 mg/mL) challenge following exposure to PBS or HDM. A: Ers average values in mice with XYM, XYF, XXF, or XXM genotypes treated with HDM or PBS. B: Ers average values in the XY or XX mice treated with HDM or PBS. C: Ers average values in the mice with male and female gonads treated with HDM or PBS. D: Rn average values in mice with XYM, XYF, XXF, or XXM genotypes treated with HDM or PBS. E: Rn average values in XY or XX mice treated with HDM or PBS. F: Rn average values in the mice with male and female gonads treated with HDM or PBS. Fixed effects included dose, treatment (PBS vs. HDM), and either sex chromosome, gonadal sex, or genotype, plus all two- and three-way interaction terms. Significant interactions were followed by pairwise estimated marginal means (EMMs) comparisons using Tukey's multiple-comparison adjustment. Significance was set at $P < 0.05$. Data represented as means \pm SD, $n = 5$ –11 mice per treatment group. * $P < 0.05$; ** $P < 0.001$, *** $P < 0.0001$ PBS of each (HDM effect). FCG, four core genotype; HDM, house dust mite; PBS, phosphate-buffered saline.

with male gonads showed significantly elevated Ers at the 100 mg/mL MCh dose compared with PBS-treated mice with male gonads ($P = 0.001$), irrespective of chromosomal composition (Fig. 1C). At 50 mg/mL and 100 mg/mL MCh doses, Ers was significantly higher in HDM-treated XX-mice compared with both PBS-treated XX mice ($P = 0.023$ and <0.0001 , respectively). In HDM-treated XY mice, Ers was only significantly increased at the 50 mg/mL dose ($P = 0.014$; Supplemental Fig. S8, A–D).

The average conducting airway resistance (Rn) values for the HDM-treated mice at 100 mg/mL were 0.735 ± 0.144 cmH₂O·s/mL for XXF, 0.847 ± 0.146 cmH₂O·s/mL for XXM, 0.718 ± 0.080 cmH₂O·s/mL for XYF, and 0.692 ± 0.094 cmH₂O·s/mL for XYM mice, respectively (Fig. 1D). The XXM mice exhibited significantly elevated Rn at 50 mg/mL of MCh in HDM-treated mouse groups compared with the other genotypes ($P = 0.013$). We did not observe significant differences in airway resistance (Rn) among the genotypes at the different doses of MCh (Supplemental Fig. S9, A–D). The XX-mice had significantly elevated Rn only at 100 mg/mL ($P = 0.029$) in the HDM-treated group compared with the PBS-treated group (Fig. 1E). Further analysis revealed that Rn was significantly higher in HDM-treated mice with female gonads at 100 mg/mL MCh doses compared with PBS-treated mice with female gonads ($P = 0.008$; Fig. 1F). In models assessing the effects of treatment, gonadal sex, sex chromosomes, genotype, and MCh dose on measured outcomes, several significant interactions and main effects were observed. In the model including treatment, gonadal sex, and dose, with all two-way and three-way interactions, the independent effects of HDM treatment ($P = 0.001$) and dose ($P < 0.001$) were statistically significant, along with the two-way interaction between gonadal sex and dose ($P < 0.001$). In the model with HDM treatment, genotype, and dose, the three-way interaction was not significant. However, the two-way interactions between genotype and dose were significant ($P < 0.001$), including the independent effects of treatment ($P = 0.002$) and dose ($P < 0.001$). In the model including treatment, sex chromosomes, and dose, significant two-way interactions were observed between sex chromosomes and dose ($P = 0.003$) and in the independent effects of treatments and dose ($P = 0.003$ and <0.001 , respectively). In XXM mice, tissue resistance (G) values at 12.5, 25, 50, and 100 mg/mL MCh doses were significantly lower in PBS-treated groups compared with HDM-treated groups ($P = 0.006$, <0.0001 , <0.0001 , and <0.0001 , respectively; Supplemental Fig. S10, A–D and Supplemental Fig. S12, A–C). In XX-mice, regardless of gonadal type, G values at 50 mg/mL and 100 mg/mL MCh doses were significantly lower in PBS-treated groups compared with HDM-treated groups ($P = 0.002$ and <0.0001 , respectively). A similar trend was observed in mice with male gonads, irrespective of sex chromosomes at 12.5, 25, 50, and 100 mg/mL doses ($P = 0.007$, <0.0001 , <0.0001 , and <0.0001 , respectively). Also, the HDM-treated XX-mice showed significantly higher G values at 25, 50, and 100 mg/mL doses of MCh compared with the HDM-treated XY-mice ($P = 0.036$, <0.001 , and <0.0001 , respectively). Among HDM-treated groups, G values in XXM mice were significantly higher at 25, 50, and 100 mg/mL MCh doses compared with XYF ($P = 0.001$, <0.0001 , and <0.0001 , respectively) and XYM mice ($P = 0.008$, <0.0001 , <0.0001 , respectively). In addition, HDM-treated mice with female gonads exhibited significantly higher G values at 25, 50, and

100 mg/mL MCh doses compared with those with male gonads ($P = 0.013$, <0.0001 , and <0.0001 , respectively). Across models evaluating the roles of treatment, MCh dose, and biological variables, namely gonadal sex, genotype, and sex chromosomes, several significant findings were observed. In the model incorporating treatment, gonadal sex, and dose, both treatment ($P = 0.002$) and dose ($P < 0.001$) showed independent significant effects, with notable two-way interactions between treatment and dose ($P < 0.001$), gonadal sex and dose ($P < 0.001$), and gonadal sex and treatment ($P = 0.004$). Interestingly, the three-way interaction among the three variables was also significant ($P < 0.001$). When genotype was included instead of gonadal sex, the three-way interaction between treatment, genotype, and dose was significant ($P < 0.001$), alongside two-way interactions between genotype and dose, treatment and dose, and treatment and genotype ($P < 0.001$, <0.001 , and <0.003 , respectively), and significant main effects of treatment ($P = 0.004$) and dose ($P < 0.001$). In a parallel model including sex chromosomes, significant two-way interactions were found between treatment and dose ($P < 0.001$) and between sex chromosomes and dose ($P < 0.001$). The independent effect of treatment and dose was also significant in this model ($P = 0.003$ and <0.001 , respectively). Notably, Rn comparisons at some doses were influenced by higher baseline Rn in XY-PBS mice, which contributed to apparent genotype differences in relative change. We therefore emphasized dose-dependent within-treatment comparisons (HDM vs. PBS) and the significant interactions reported by the mixed models when interpreting Rn results.

Tissue elastance (H) was also evaluated in FCG mice following allergen exposure (Supplemental Fig. S11, A–D and Supplemental Fig. S12, D–F). In XXM genotype mice, HDM-treated groups exhibited significantly higher H values at 25, 50, and 100 mg/mL MCh doses compared with PBS-treated groups ($P = 0.029$, <0.0001 , and <0.0001 , respectively; Supplemental Fig. S11B). Within the HDM-treated groups, XXM mice at 50 and 100 mg/mL MCh doses showed significantly greater H values compared with XYM genotypes ($P = 0.036$ and <0.0001) and XYF ($P = 0.048$ and <0.0001). In XX-mice, irrespective of gonadal sex, H values were significantly higher at 25, 50, and 100 mg/mL MCh doses in HDM-treated groups compared with PBS-treated groups ($P = 0.015$, <0.0001 , and <0.0001). Furthermore, at 50 and 100 mg/mL MCh doses, HDM-treated XX mice exhibited higher H values than XY-treated mice ($P = 0.008$ and <0.0001). In HDM-treated mice with male gonads, H values were significantly higher at 25, 50, and 100 mg/mL MCh doses compared with PBS-treated counterparts ($P = 0.024$, <0.001 , and <0.0001 , respectively). Also, at the 100 mg/mL MCh dose, HDM-treated male gonad mice had higher H values than their female counterparts ($P = 0.029$). In models evaluating the roles of treatment, methacholine (MCh) dose, and biological variables, including gonadal sex, genotype, and sex chromosomes, several significant findings emerged. In the model incorporating treatment, gonadal sex, and dose, both treatment ($P = 0.009$) and dose ($P < 0.001$) showed significant independent effects, with notable two-way interactions between treatment and dose ($P = 0.003$) and gonadal sex and dose ($P = 0.021$). The

Three-way interactions for these variables were also significant ($P = 0.011$). When genotype was included instead of gonadal sex, the three-way interaction between treatment, genotype, and dose was significant ($P = 0.004$), alongside two-way interactions between genotype and dose and treatment and dose (both P values < 0.001), and significant independent effects of treatment ($P = 0.004$) and dose ($P < 0.001$). In a parallel model including sex chromosomes, significant two-way interactions were found between treatment and dose ($P < 0.001$) and between sex chromosomes and dose ($P < 0.001$). The three-way interactions among the variables were significant ($P < 0.001$), including the independent effects of treatment and dose at $P \leq 0.001$. Although the magnitude of MCh-induced changes was modest relative to some HDM models, the significant increases in resistance and elastance confirm successful induction of allergic airway inflammation. This moderate phenotype was optimal for detecting sex- and genotype-dependent variations.

Histological changes.

Histopathological examination of lung tissues revealed inflammation of the peribronchial area, perivascular area, and goblet cells hyperplasia of the lung tissue in HDM-treated FCG mice compared with the PBS-treated group (Fig. 2, A–K). Peribronchial inflammation was significantly elevated only in HDM-induced XYF mice when compared with PBS-treated controls of the same genotype ($P = 0.004$; Fig. 2A). When stratified by sex chromosome complement, HDM-treated mice carrying either XX or XY chromosomes, regardless of gonadal sex, displayed significantly greater peribronchial inflammation than their respective PBS-treated counterparts ($P = 0.023$ and 0.043 , respectively; Fig. 2B). In contrast, when grouped by gonadal sex irrespective of chromosomal sex, a significant increase in peribronchial inflammation was observed only in HDM-treated mice with female gonads compared with PBS controls ($P = 0.003$; Fig. 2C). In the statistical model incorporating HDM treatment, gonadal sex, and all two-way interaction terms, the independent effect of treatment was the only significant factor ($P = 0.003$). A similar trend was observed in the model analyzing treatment and sex chromosome complement, where treatment again remained the sole significant predictor of peribronchial inflammation ($P = 0.023$). Perivascular inflammation was elevated across all HDM-treated genotypes compared with PBS-treated controls, with significant increases observed in XYF ($P < 0.0001$), XXF ($P = 0.009$), and XXM ($P = 0.040$) mice, whereas the XYM group did not show a statistically significant difference (Fig. 2D). When grouped by sex chromosome complement, both HDM-treated XX and XY mice exhibited significantly higher perivascular inflammation relative to their PBS-treated counterparts ($P = 0.003$ and 0.005 , respectively; Fig. 2E). Similarly, grouping by gonadal sex revealed significant perivascular inflammation in HDM-treated mice with both female ($P < 0.001$) and male ($P = 0.028$) gonads, with inflammation levels significantly greater in mice with female gonads versus male gonads ($P = 0.008$; Fig. 2F). In the statistical model including treatment, gonadal sex, and their two-way interaction, both treatment ($P < 0.003$) and gonadal sex ($P = 0.001$) had significant independent effects. In the model evaluating

treatment and sex chromosome complement, treatment remained a significant predictor of perivascular inflammation ($P = 0.003$). Finally, in the model assessing treatment, genotype, and their two-way interaction, both treatment ($P = 0.009$) and genotype ($P = 0.019$) showed significant independent effects, though the interaction was not statistically significant. In HDM-treated mice, goblet cell hyperplasia was significantly elevated in mice with XX chromosomes and female gonads compared with their respective PBS-treated controls ($P = 0.026$ and 0.014 , respectively), whereas no significant differences were observed across the different genotypes (Fig. 2, G–I). Furthermore, in statistical models incorporating treatment and either the sex chromosome complement or gonadal sex, including their respective interaction terms, treatment emerged as the only factor with a significant independent effect ($P = 0.026$ and 0.014 , respectively). Notably, we observed mild peribronchial inflammation in PBS-treated XXF mice, which suggests an intrinsic immune activation associated with the XX complement and female gonads. Quantitative analysis of airway epithelial remodeling revealed genotype-, chromosome-, and gonadal sex-dependent patterns of goblet cell hyperplasia following HDM exposure (Fig. 2, L–N). HDM-treated XXF and XXM mice showed significant increases compared with their PBS-treated controls ($P < 0.05$), whereas XYF and XYM groups exhibited minimal changes. When data were grouped by chromosome complement, HDM-treated XX mice displayed markedly higher PAS+ cell counts than XY mice ($P < 0.01$), and mice with female gonads similarly demonstrated elevated PAS+ cell densities compared with those bearing male gonads ($P < 0.05$). These findings indicate that both the presence of two X chromosomes and female gonadal status enhance epithelial remodeling in response to allergen challenge, consistent with the overall trend of increased airway inflammation observed in female and XX genotypes.

Flow cytometry.

Flow cytometry analysis of lung tissue from challenged mice confirmed that multiple immune cell populations were significantly influenced by genotype, sex chromosome complement, and gonadal sex following allergen exposure (Fig. 3). We focused on quantifying immune cells in lung tissue to capture both interstitial and airway-resident populations that contribute to local inflammation. Adjusted gating thresholds were verified to account for inflammation-related Siglec-F modulation. Among these, eosinophils were significantly elevated in HDM-treated XXF mice compared with both PBS-treated XXF ($P < 0.001$) and other genotypes in the HDM-treated group (XXM, $P = 0.001$; XYM, $P = 0.003$), except for the XYF genotype (Fig. 3A). When analyzed by sex chromosome complement, HDM-treated XX mice exhibited higher eosinophil counts than XY-treated mice, though this difference did not reach statistical significance (Fig. 3B). In contrast, HDM-treated mice with female gonads had significantly higher eosinophil levels than those with male gonads ($P < 0.0001$; Fig. 3C). Furthermore, eosinophil counts were significantly elevated in HDM-treated mice with female gonads compared with their PBS-treated controls ($P < 0.0001$).

In HDM-treated mice, CD4⁺ T cell levels were significantly lower in the XXM genotype compared with the XXF group ($P = 0.001$). However, within the same treatment

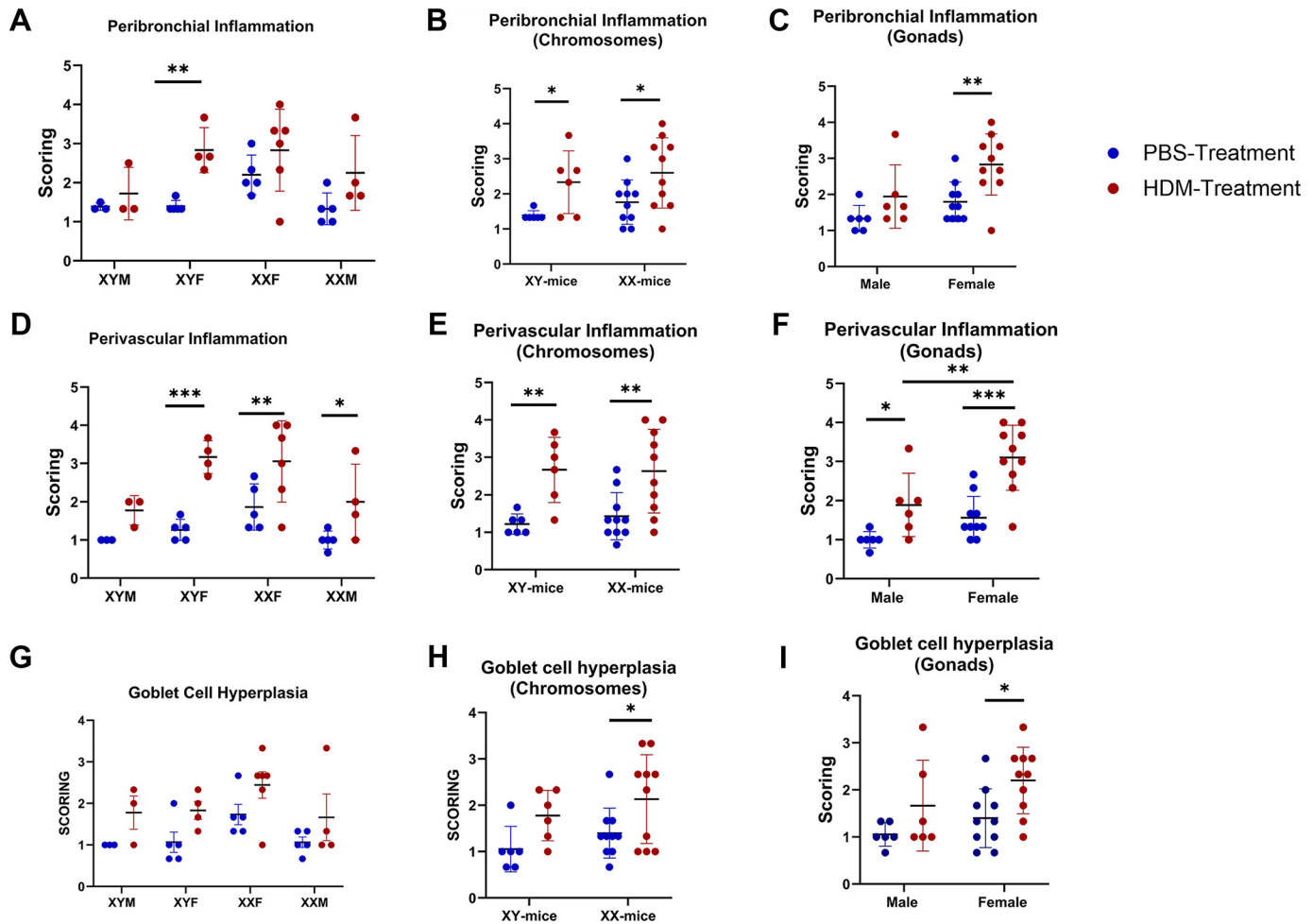


Figure 2. Histopathological analyses of lung tissue from four core genotype (FCG) mice following 5 wk of HDM or PBS exposure. Graphs represent semi-quantitative scoring for peribronchial inflammation by genotype (XYM, XYF, XXF, and XXM) (A), chromosome complement (XY vs. XX) (B), and gonadal sex (male vs. female) (C); and perivascular inflammation by genotype (D), chromosome complement (E), and gonadal sex (F). Goblet cell hyperplasia is shown by genotype (G), sex chromosome complement (H), and gonadal sex (I). Representative histological images demonstrate inflammation and epithelial remodeling across genotypes: Hematoxylin and eosin (H&E)-stained lung sections showing peribronchial and perivascular inflammatory cell infiltration (black arrows; J); and Alcian Blue/Periodic Acid-Schiff (AB-PAS)-stained sections showing PAS-positive goblet cells (black arrows) along the airway epithelium (K). Scale bars: 200 μm (J–K). Quantitative analysis of PAS-positive goblet cells is shown, normalized to airway basement membrane area (cells/ mm^2), by genotype (L), sex chromosome complement (M), and gonadal sex (N). Statistical analyses were performed using standard linear regression models to assess the effects of treatment, sex chromosome complement, gonadal sex, and genotype, including two-way interaction terms. Type III sums of squares were applied to determine main-effect significance, and Tukey-adjusted pairwise estimated marginal means (EMMs) were calculated for multiple comparisons. Data are presented as means \pm SD ($n = 3\text{--}5$ mice/group). * $P < 0.05$; ** $P < 0.001$ denote statistical significance. Note: Mild elevations observed in XXF PBS mice represent nonpathological baseline variation consistent with intrinsic biological differences rather than spontaneous inflammation. HDM, house dust mite; PBS, phosphate-buffered saline.

group, XXM mice exhibited significantly higher CD4^+ T cell counts than HDM-treated XYF mice ($P < 0.0001$; Fig. 3D). In addition, CD4^+ T cell counts were not statistically significant between XX- or XY-mice in both treatments ($P = 0.350$; Fig. 3E). On the contrary, mice with female gonads were associated with greater CD4^+ T cell counts compared with those with male gonads ($P = 0.002$) in the HDM-treated group (Fig. 3F). Similarly, HDM-treated XXF mice exhibited significantly higher CD8^+ T cell levels compared with XXM, XYF, and XYM mice ($P < 0.0001$ for all comparisons). In addition, HDM-treated XYF mice showed significantly elevated CD8^+ T cells compared with XYM mice receiving the same treatment ($P < 0.0001$; Fig. 3G). CD4^+ T and CD8^+ T cell percentages did not significantly differ between XY and XX mice across treatment groups (Fig. 3H). However, in

the HDM-treated group, mice with female gonads consistently exhibited higher levels of both CD4^+ and CD8^+ T-cells compared with those with male gonads ($P = 0.002$ and < 0.0001 , respectively; Fig. 3, F and I).

The HDM allergen challenge significantly elevated AM counts in XXM mice compared with both XYF and XYM genotypes ($P = 0.002$ each) and their respective PBS-treated controls ($P = 0.001$). However, AM counts in HDM-treated XXM mice were significantly higher than those in HDM-treated XXF mice ($P < 0.0001$) (Fig. 4A). In addition, HDM exposure led to decreased AM counts in XXF and XYM mice compared with their respective control groups ($P = 0.0032$ and 0.011 , respectively). Interestingly, HDM-treated XY mice exhibited reduced AM counts compared with their PBS-treated counterparts ($P = 0.013$; Fig. 4B). Furthermore,

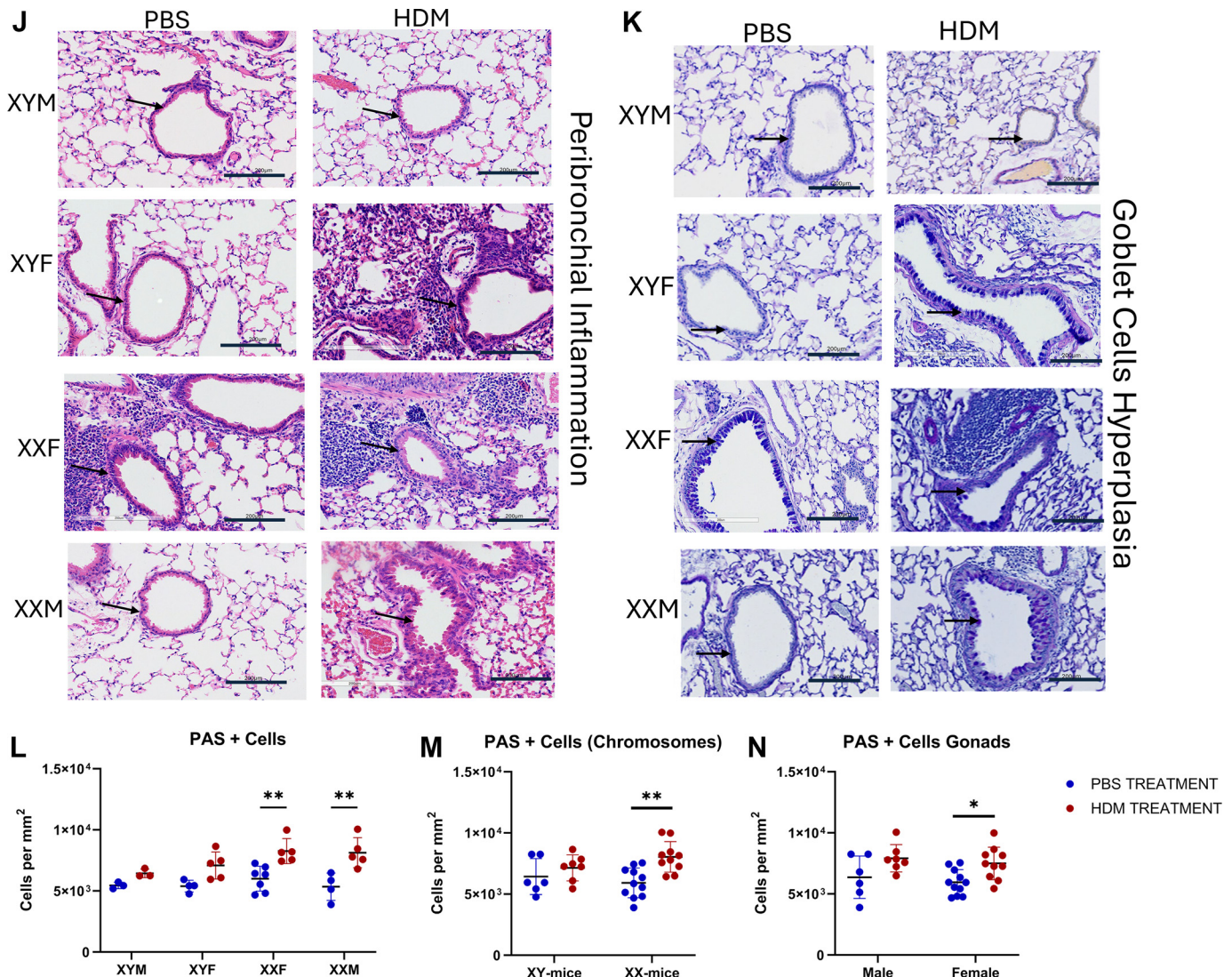


Figure 2. Continued

HDM-treated mice with female gonads had significantly lower AM counts than both HDM-treated male gonad-bearing mice ($P = 0.006$) and PBS-treated mice with female gonads ($P = 0.027$; Fig. 4C). CD103⁺ dendritic cells (DCs) were significantly enriched only in HDM-treated XXM mice compared with other HDM-treated genotypes, including XXF, XYF, and XYM ($P = 0.001$, 0.003 , and 0.001 , respectively; Fig. 4D). In addition, among HDM-treated mice, those with XX chromosomes showed higher CD103⁺ DC counts than those with XY chromosomes ($P = 0.048$; Fig. 4E), and male gonad-bearing mice had significantly higher counts than female gonad-bearing counterparts ($P = 0.032$; Fig. 4F). Plasmacytoid dendritic cells (pDCs) were significantly increased in HDM-treated XYM mice compared with XXF, XXM, and XYF genotypes ($P < 0.0001$, 0.026 , and 0.0001 , respectively; Fig. 5A). Furthermore, HDM-treated mice with female gonads exhibited lower pDC counts than those with male gonads ($P = 0.001$; Fig. 5B). HDM-treated XYM mice exhibited a significant increase in CD11b⁺ DC counts compared with their PBS-treated controls ($P = 0.006$; Fig. 5C). When analyzed by sex chromosome complement, HDM-

treated XY mice showed significantly higher CD11b⁺ DC counts than both XX mice ($P = 0.006$) and XY mice in the PBS-treated group ($P = 0.003$; Fig. 5D).

Interestingly, HDM treatment did not lead to significant changes in B cell counts across all genotypes (Supplemental Fig. S13A). However, when comparing genotypes, B cells were significantly elevated in HDM-treated XYM mice compared with XXF mice ($P = 0.004$), and counts were higher in mice with male gonads than those with female gonads ($P = 0.014$; Supplemental Fig. S13B). Interstitial macrophages were significantly reduced in XXM mice compared with XYF mice ($P = 0.007$), although no significant differences were observed between control and HDM-treated groups within any genotype (Supplemental Fig. S13C). Undifferentiated monocytes, neutrophils, NKT cells, and NK cells showed no significant differences between treatment groups across all genotypes (Supplemental Fig. S13, D–M).

In the model evaluating the effects of sex chromosome complement and treatment, along with their two-way interaction, treatment independently influenced eosinophil counts ($P = 0.018$), while sex chromosome complement

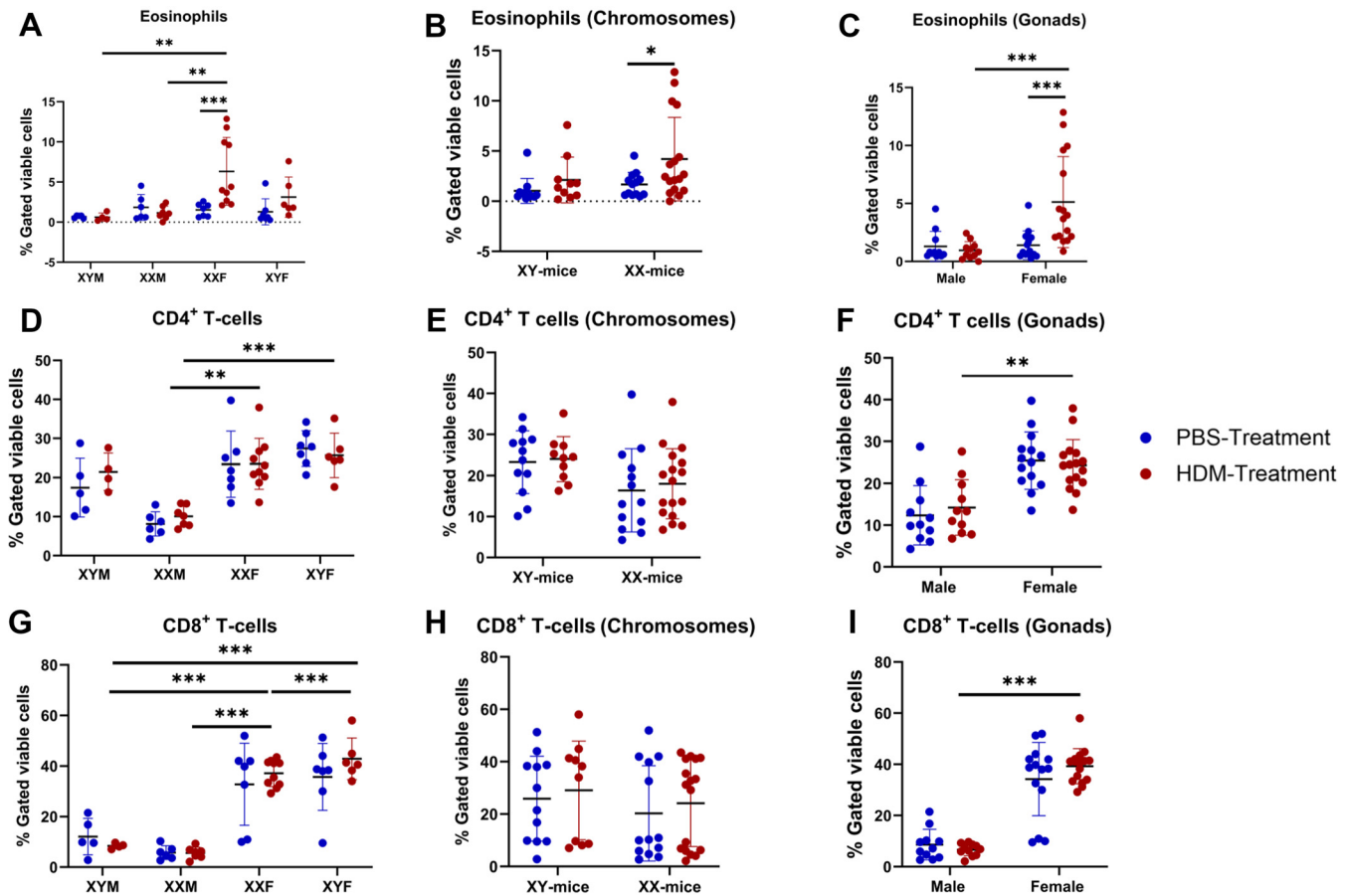


Figure 3. The percentages of eosinophils in the lungs of XYM, XYF, XXF or XXM genotype mice (A), eosinophils in the lungs of XY or XX mice (B), eosinophils in the lungs of male or female gonadal sex mice (C), CD4⁺ T-cells in the lungs of XYM, XYF, XXF or XXM genotype mice (D), CD4⁺ T-cells in the lungs of XY or XX mice (E), CD4⁺ T-cells in the lungs of male or female gonadal sex mice (F), CD8⁺ T-cells in the lungs of XYM, XYF, XXF or XXM genotype mice (G), CD8⁺ T-cells in the lungs of XY or XX mice (H), CD8⁺ T-cells in the lungs of male or female gonadal sex mice (I), ($n = 4-8$ mice/group). Results shown as graphs and flow cytometry plots depict average cell percentages (percent of live cells). Linear regression models were applied to assess independent and interaction effects of treatment, sex chromosomes, gonadal sex, and genotype on immune-cell percentages. Where overall effects were significant, pairwise EMMs were compared with Tukey correction for family-wise error. Error bars denote SD. All gates were defined using FMO controls to account for Siglec-F expression variability under naïve and inflamed conditions. Full antibody validation and gating strategies are available in reference (46). * $P < 0.05$, ** $P < 0.001$, *** $P < 0.0001$. EMM, estimated marginal mean; FMO, fluorescence minus one.

independently influenced the populations of CD11b⁺ DCs ($P = 0.001$), AMs ($P = 0.012$), CD103⁺ DCs ($P = 0.01$), interstitial macrophages ($P = 0.03$), and CD4⁺ T cells ($P = 0.026$). The interaction between sex chromosome and treatment was significant in influencing CD11b⁺ DC ($P = 0.019$) and AM populations ($P = 0.017$). On the contrary, in the model incorporating gonadal sex and treatment, including their interaction, gonadal sex independently influenced the populations of CD103⁺ DCs ($P = 0.007$), eosinophils ($P < 0.001$), B cells ($P = 0.003$), NK cells ($P = 0.023$), NKT cells ($P = 0.029$), plasmacytoid DCs ($P < 0.001$), CD8⁺ T-cells ($P < 0.001$), CD4⁺ T-cells ($P < 0.001$), and AMs ($P = 0.001$). Treatment also independently affected AMs ($P = 0.027$) and eosinophils ($P < 0.001$). The interaction between gonads and treatment was significant for AMs ($P = 0.025$) and eosinophils ($P = 0.004$). Finally, in the model including genotype and treatment with their interaction, genotype independently influenced CD4⁺ T-cells ($P < 0.001$), CD8⁺ T-cells ($P < 0.001$), plasmacytoid DCs ($P < 0.001$), AMs ($P < 0.001$), B cells ($P = 0.001$), CD11b⁺ DCs ($P = 0.011$), eosinophils ($P <$

0.001), and CD103⁺ DCs ($P < 0.001$). Treatment also independently influenced AMs ($P = 0.032$) and eosinophils ($P < 0.001$), and the interaction effect was also significant for eosinophils ($P = 0.012$) and AMs ($P < 0.001$). Across all models, neutrophils and undifferentiated monocytes showed no significant changes in response to treatment, genotype, sex chromosome, or gonadal sex.

DISCUSSION

This study provides compelling evidence that airway hyperresponsiveness (AHR), immune cell infiltration, and inflammatory histopathology in response to allergen exposure are significantly influenced by sex chromosome complement, gonadal sex, and genotype in a four-core genotype (FCG) mouse model. Using the HDM challenge, we observed clear genotype-specific differences in lung function parameters, immune profiles, and histological markers of inflammation, advancing our understanding of how sex-based biological factors modulate allergic airway disease.

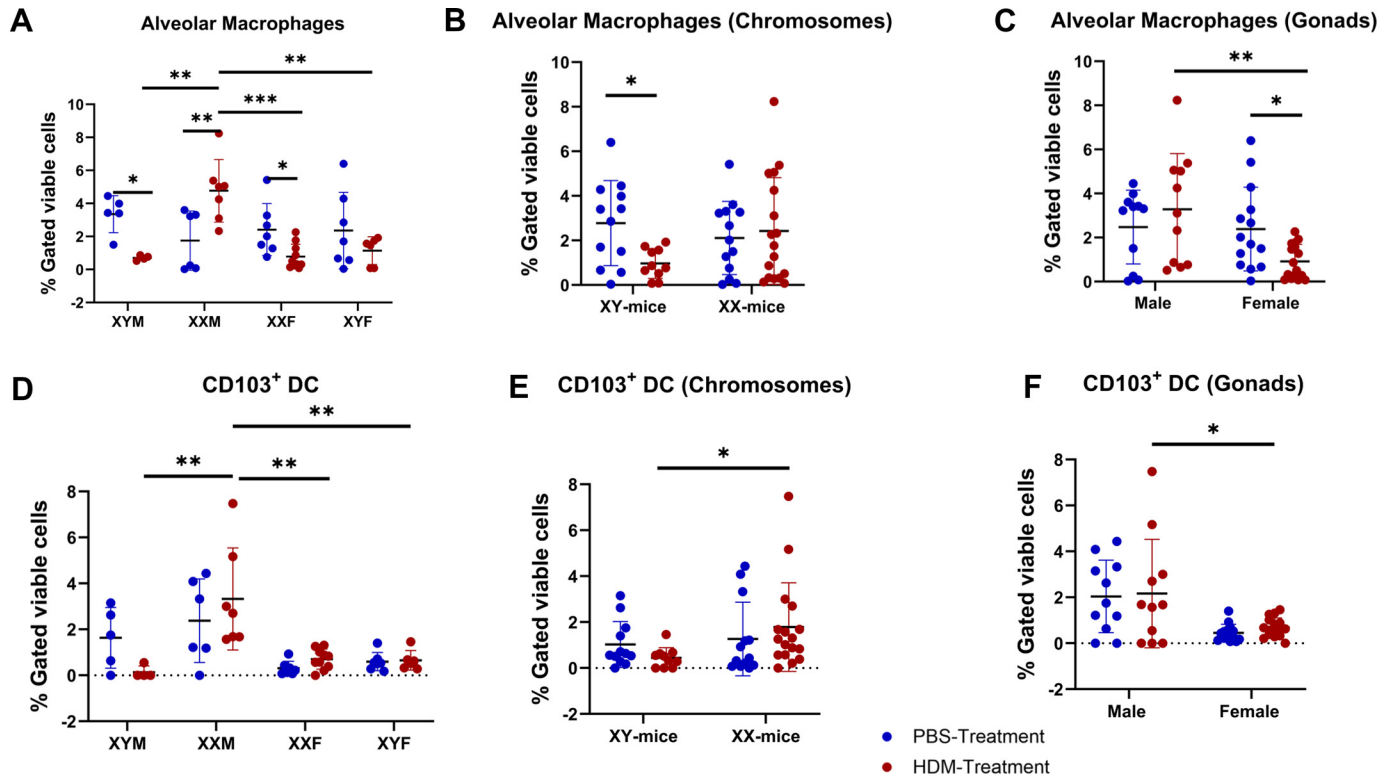


Figure 4. The percentages of alveolar macrophages in the lungs of XYM, XYF, XXF or XXM genotype mice (A), alveolar macrophages in the lungs of XY or XX mice (B), alveolar macrophages in the lungs of male or female gonadal sex mice (C), $CD103^{+}$ DC in the lungs of XYM, XYF, XXF, or XXM genotype mice (D), $CD103^{+}$ DC in the lungs of XY or XX mice (E), $CD103^{+}$ DC in the lungs of male or female gonadal sex mice (F) ($n = 4-8$ mice/group). Results shown as graphs and flow cytometry plots depict average cell percentages (percent of live cells). Linear regression models tested the effects of treatment, genotype, sex chromosome complement, and gonadal sex, including their interactions. Significant interactions were decomposed by EMM contrasts with Tukey's post hoc adjustment. $P < 0.05$ indicates statistical significance. Error bars denote SD. * $P < 0.05$, ** $P < 0.001$, *** $P < 0.0001$. DC, dendritic cell; EMM, estimated marginal mean.

In terms of lung function, HDM challenge resulted in a dose-dependent increase in all measured parameters (Rrs, Ers, Rn, G, and H), with notable differences among FCG mice. This finding is consistent with previous studies demonstrating that genetic factors can influence AHR, particularly in response to environmental allergens (52–54). The XXM genotype consistently exhibited the highest airway resistance (Rrs) and lung elastance (Ers) following HDM exposure. This aligns with the well-established association between allergen-induced inflammation and AHR (55, 56), while XYM mice showed the lowest values. This divergence highlights the complex interplay between chromosomal and gonadal influences on airway mechanics (52–54). Notably, a XX chromosomal complement, regardless of gonadal sex, was associated with significantly elevated Ers and Rrs, suggesting that gene dosage effects or X-linked immune-modulatory genes may exacerbate airway reactivity (57), aligning with our previous study, in which AHR was greater in male than in female animals (58).

Histopathological analysis revealed significant alterations in the lung tissue of HDM-treated mice, including peribronchial and perivascular inflammation and goblet cell hyperplasia, with differences influenced by genotype, sex chromosomes, and gonadal sex. These changes are hallmark features of asthma pathogenesis (59–62). Notably, the enlargement of the perivascular region was significant in HDM-treated mice across all genotypes, except in XYM mice,

compared with their respective controls. The lack of widespread, significant histological changes across genotypes may be due to the duration of allergen exposure, the type and route of allergen administration, or the inherent variability in histopathological responses among genetically distinct mice (63–65). However, a similar finding was reported in a recently published article from our laboratory (57), in which inflammatory gene expression was greater in female mice than in male mice exposed to allergens. Overall, female gonad and XX-mice groups exhibited greater inflammation, particularly perivascular and goblet cell hyperplasia, while treatment effects were consistently significant across all parameters ($P < 0.05$). HDM-treated mice with female gonads exhibited significantly increased perivascular inflammation compared with those with male gonads, consistent with previous findings showing that females tend to have a more pronounced inflammatory response to allergens (58, 66, 67). The increased inflammation and tissue changes observed in mice with female gonads further emphasize that female gonadal sex may drive heightened airway inflammation through hormonal regulation of immune effectors and epithelial remodeling. This is further supported by the elevated eosinophilic infiltration in HDM-treated mice with female gonads, a hallmark feature of type 2-driven asthma.

Immune cell profiling assessed by flow cytometry also revealed significant differences in the populations of AMs, eosinophils, and DCs across genotypes in response to HDM

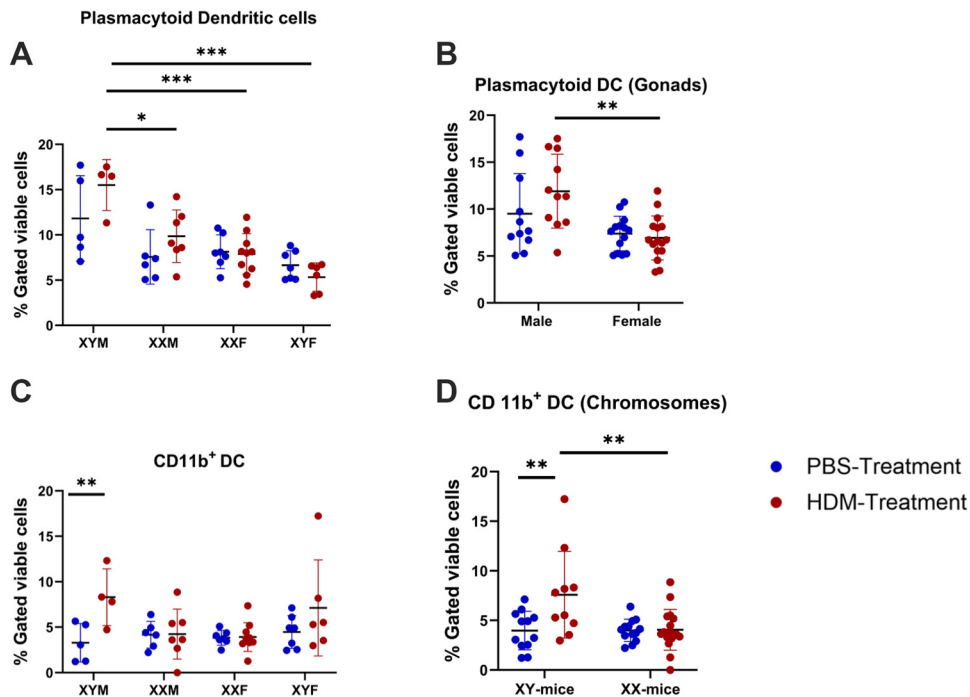


Figure 5. The percentages of plasmacytoid DC in the lungs of XYM, XYF, XXF, or XXM genotype mice (A), plasmacytoid DC in the lungs of male or female gonadal sex mice (B), CD11b⁺ DC in the lungs of XYM, XYF, XXF, or XXM genotype mice (C), CD11b⁺ DC in the lungs of XY or XX mice (D), ($n = 4-8$ mice/group). Results shown as graphs and flow cytometry plots depict average cell percentages (percent of live cells). Linear regression models evaluated treatment, genotype, and sex variables with Type III sums of squares. When significant main or interaction effects were detected, pairwise group differences were assessed via Tukey-adjusted EMM comparisons. Error bars denote SD. * $P < 0.05$, ** $P < 0.001$, *** $P < 0.0001$. DC, dendritic cell; EMM, estimated marginal mean.

exposure. We found that genotype, sex chromosomes, and gonadal sex significantly influenced immune cell populations in the lungs of FCG mice after allergen exposure. Alveolar macrophages were significantly elevated in XXM mice, suggesting a heightened innate immune response in this genotype. This finding is consistent with studies indicating that macrophage activation plays a crucial role in asthma exacerbations (68, 69). Eosinophils, which are key mediators of allergic inflammation in asthma (70, 71), were significantly elevated in XXF mice, bearing both female gonads and chromosomes. Interestingly, the interaction between genotype and treatment appeared to influence immune cell populations in a complex manner: certain subsets, such as DCs, showed a strong genotype-dependent response to HDM exposure, whereas others, such as neutrophils, did not show significant differences. This underscores the complex nature of immune cell responses in allergic asthma, which can vary based on genetic background and sex chromosome complement (72). Specific genotypes exhibited distinct immune responses: XXM mice showed elevated AMs and CD103⁺ DCs; XXF mice showed increased eosinophils and CD8⁺ T-cells; and XYM mice showed heightened plasmacytoid DCs and CD11b⁺ DCs. Similarly, sex chromosomes influenced immune cell responses, with XY mice showing elevated CD11b⁺ DCs and reduced CD103⁺ DCs compared with XX mice. Gonadal sex also influenced this phenotype, with female gonad mice exhibiting higher eosinophil, CD4⁺, and CD8⁺ T cell counts, while male gonad mice had higher AMs, CD103⁺ DCs, and plasmacytoid DCs. Analysis of DC subsets in the lung revealed a local antigen-presenting cell composition distinct from migratory lymph node populations (72). MHC II expression was incorporated into our gating of DCs and interstitial macrophages. These findings emphasize the complex interplay between genetic and biological factors in shaping immune responses to allergens, with significant independent

and interaction effects observed across treatments and immune cell types. Using lung tissue rather than lavage enabled us to focus on tissue-resident immune populations critical for sustained inflammation. The potential modulation of Siglec-F during inflammation was accounted for in the gating strategy validation, ensuring reliable quantification of AMs and eosinophils.

Although DCs migrate to draining lymph nodes to prime adaptive responses, quantifying their numbers within lung tissue provides insight into local antigen-presenting activity and inflammatory recruitment. CD103⁺ and CD11b⁺ DC subsets act as critical sentinels within the airway mucosa, and their differential abundance among genotypes in our study likely reflects distinct local immune activation patterns rather than migratory endpoints. This local perspective complements systemic immune profiling and helps delineate genotype- and gonadal sex-specific contributions to antigen sensing and presentation within the lung.

One of the central findings of this study was the significant contribution of both sex chromosomes and gonadal sex in modulating the inflammatory response to allergen exposure. Although previous research has emphasized the role of gonadal hormones in modulating asthma pathogenesis (73, 74), this study highlights the importance of sex chromosome complement in this modulation. The XXM genotype exhibited the most pronounced responses across multiple measures of airway function and histology, suggesting a significant role for the X chromosome in asthma phenotypes. Conversely, the gonadal sex influence was particularly notable in the histological assessment, where mice with female gonads displayed more pronounced tissue changes in the peribronchial and perivascular regions. These results are in line with prior studies suggesting that estrogen and other ovarian hormones may enhance the allergic response in female mice (75-77).

The moderate phenotype observed after five weeks of HDM exposure is consistent with controlled and reproducible models of allergic inflammation that are designed to uncover subtle, yet biologically meaningful, sex- and genotype-dependent effects. Although we did not quantify structural remodeling markers such as collagen deposition or airway smooth muscle hypertrophy, both physiological and histological evidence confirmed the presence of inflammatory remodeling. The MCh challenge revealed distinct genotype-dependent effects on airway resistance and lung elastance, with XXM mice exhibiting the most pronounced responses, particularly at higher doses. Histological analyses further demonstrated significant alterations in lung architecture, including peribronchial and perivascular inflammation, epithelial thickening, and goblet cell proliferation. These changes were more evident in mice with female gonads, suggesting hormonal modulation of airway remodeling. Quantitative assessment of PAS-positive epithelial cells normalized to airway number supported the semiquantitative histological scores, revealing modest but nonsignificant increases in goblet cell numbers after HDM exposure. Although goblet cell hyperplasia was limited under the present experimental conditions, more refined morphometric approaches, such as airway area-normalized counts and differentiation between acidic and neutral mucins, may enhance sensitivity for detecting subtle epithelial changes.

Future studies will incorporate MUC5AC and MUC5B immunostaining and evaluate the expression of epithelial lineage markers (*Foxj1*, *Scgb1a1*, and *Spdef*) to further define mucin subtype regulation and epithelial differentiation in relation to sex chromosome and gonadal influences. Of note, a modest increase in peribronchial and perivascular inflammation and goblet cell presence was observed in PBS-treated XXF mice relative to other control groups. This finding likely reflects a mild baseline immune activation driven by the combined effects of the XX chromosomal complement and the female gonadal environment. Consistent with this interpretation, prior studies using the four core genotype model, including our recent transcriptomic analysis (42) have shown that XXF mice exhibit higher basal expression of inflammatory and epithelial differentiation genes, indicative of an intrinsically heightened immune tone. Thus, the mild histological changes observed in XXF PBS mice are best explained by low-level epithelial priming rather than spontaneous airway inflammation.

Flow cytometry analyses further demonstrated genotype-dependent variations in immune cell populations, including elevated AMs and eosinophils, as well as gonadal sex-associated effects on eosinophil and T-cell responses. These findings underscore the importance of both chromosomal and hormonal factors in shaping immune cell composition and activation during allergic inflammation.

This study has some limitations. First, the house dust mite (HDM) dosing regimen used here (25 μ g intranasally, 5 days/wk for 5 wk) was selected to induce a reproducible but moderate allergic airway phenotype that preserves sensitivity to sex chromosome and gonadal-dependent effects. Although this approach avoids ceiling effects that can obscure biological differences, it may not fully recapitulate progressive or severe asthma phenotypes characterized by

extensive airway remodeling and exaggerated airway hyperresponsiveness. Future studies employing higher-dose, intermittent, or exacerbation-based HDM paradigms, as well as longitudinal designs, will be important for modeling asthma progression and sex-specific disease trajectories. Second, immune cell profiling was performed using whole lung tissue rather than bronchoalveolar lavage (BAL) to allow simultaneous evaluation of airway wall and parenchymal compartments. Although this approach provides a comprehensive assessment of tissue-resident immune populations, it limits direct comparison with luminal inflammatory responses. Future studies combining tissue and BAL analyses will enable a more complete understanding of immune cell localization, activation, and trafficking. Third, although we provide a detailed phenotypic characterization of dendritic cell (DC) subsets within lung tissue, the present study does not assess DC migration to draining mediastinal lymph nodes or directly examine costimulatory activation markers such as CD86. Although MHC II-defined DC populations inform local antigen-presenting cell distribution within the lung, future work will be required to establish mechanistic links between sex differences, DC trafficking, and downstream adaptive immune responses. Finally, airway remodeling was evaluated primarily through semiquantitative histological scoring and PAS-positive goblet cell enumeration. We did not directly quantify airway smooth muscle mass, collagen deposition, or the expansion of specific epithelial cell subsets. Incorporation of α -smooth muscle actin and collagen staining, as well as mucin-specific and epithelial lineage markers (e.g., MUC5AC, MUC5B), will allow a more comprehensive assessment of sex-dependent airway remodeling. Although sample sizes were adequate to detect sex- and genotype-dependent differences in key physiological and immune parameters, larger cohorts may be required to capture subtler aspects of epithelial remodeling. Despite these limitations, the present study establishes a strong experimental framework for dissecting the independent and interactive roles of sex chromosomes and gonadal sex in allergic airway inflammation.

Collectively, our findings highlight the complex interplay between sex chromosome complement and gonadal sex in regulating airway inflammation, immune cell dynamics, and tissue remodeling following allergen exposure. These results provide mechanistic insight into the well-documented sex bias in asthma prevalence and severity, wherein females experience heightened inflammation and airway hyperresponsiveness during reproductive years. The demonstration that both chromosomal and hormonal factors contribute to immune regulation suggests that variations in either domain, such as those occurring in Turner syndrome (XO), Klinefelter syndrome (XXY), androgen insensitivity, menopause, or andropause, may alter asthma susceptibility and disease course.

In conclusion, understanding how sex chromosomes and gonadal hormones independently and jointly influence pulmonary immune function offers an important framework for developing sex-informed therapeutic strategies. Future studies translating these findings to human cohorts with defined chromosomal or hormonal alterations could further elucidate the biological drivers of asthma heterogeneity and improve precision medicine approaches for airway disease.

DATA AVAILABILITY

All sources of data can be found at: <https://doi.org/10.17605/OSF.IO/UC7JN>.

SUPPLEMENTAL MATERIAL

Supplemental Figs. S1–S13 are available at: <https://doi.org/10.6084/m9.figshare.30585662>.

ACKNOWLEDGMENTS

The authors thank the Indiana University Bloomington Flow Cytometry Core Facility (IUB FCCF) for the use of its instrumentation and technical expertise. The CytoFLEX LX flow cytometer used in this study was funded in part by the IU Office of Research through the Research Equipment Fund.

GRANTS

This study was supported by NIH/NHLBI, Grant/Award Number R01HL159764, and the Indiana Clinical and Translational Sciences Institute, which is funded in part by Award Number UM1TR004402 from the National Institutes of Health, National Center for Advancing Translational Sciences, Clinical and Translational Sciences Award.

DISCLAIMERS

The content is solely the responsibility of the authors and does not necessarily represent the official views of the National Institutes of Health.

DISCLOSURES

No conflicts of interest, financial or otherwise, are declared by the authors.

AUTHOR CONTRIBUTIONS

C.D.E. and P.S. conceived and designed research; C.D.E., D.R., R.A., O.B.-S., M.B., S.S., L.D., and P.S. performed experiments; E.P. analyzed data; C.D.E., S.B., M.L.R., and P.S. interpreted results of experiments; C.D.E., E.P., and P.S. prepared figures; C.D.E. and P.S. drafted manuscript; C.D.E., D.R., R.A., O.B.-S., M.B., S.S., L.D., E.P., and P.S. edited and revised manuscript; C.D.E., D.R., R.A., O.B.-S., M.B., S.S., L.D., E.P., and P.S. approved final version of manuscript.

REFERENCES

- Mohan A, Ludwig A, Brehm C, Lugogo NL, Sumino K, Hanania NA. Revisiting mild asthma: current knowledge and future needs. *Chest* 161: 26–39, 2022. doi:10.1016/j.chest.2021.09.004.
- GBD 2019 Diseases and Injuries Collaborators. Global burden of 369 diseases and injuries in 204 countries and territories, 1990–2019: a systematic analysis for the Global Burden of Disease Study 2019. *Lancet* 396: 1204–1222, 2020 [Erratum in *Lancet* 396: 1562, 2020]. doi:10.1016/S0140-6736(20)30925-9.
- The Global Asthma Report 2022. *Int J Tuberc Lung Dis* 26: 1–104, 2022. doi:10.5588/ijtld.22.1010.
- Halonon M, Stern DA, Lohman C, Wright AL, Brown MA, Martinez FD. Two subphenotypes of childhood asthma that differ in maternal and paternal influences on asthma risk. *Am J Respir Crit Care Med* 160: 564–570, 1999. doi:10.1164/ajrccm.160.2.9809038.
- Sharma S, Kho AT, Chhabra D, Haley K, Vyhlidal C, Gaedigk R, Leeder JS, Tantisira KG, Raby B, Weiss ST. Effect of intrauterine smoke exposure on microRNA-15a expression in human lung development and subsequent asthma risk. *Healthcare (Basel)* 8: 536, 2020. doi:10.3390/healthcare8040536.
- Hamid QA, Minshall EM. Molecular pathology of allergic disease: I: lower airway disease. *J Allergy Clin Immunol* 105: 20–36, 2000. doi:10.1016/S0091-6749(00)90172-6.
- Gandhi VD, Davidson C, Asaduzzaman M, Nahirney D, Vliagoftis H. House dust mite interactions with airway epithelium: role in allergic airway inflammation. *Curr Allergy Asthma Rep* 13: 262–270, 2013. doi:10.1007/s11882-013-0349-9.
- Zerk J-P, Heinrich J, Jarvis D, Verlato G, Norbäck D, Plana E, Sunyer J, Chinn S, Olivieri M, Soon A, Villani S, Ponzio M, Dahlman-Hoglund A, Svanes C, Luczynska C; Indoor Working Group of the European Community Respiratory Health Survey II. Distribution and determinants of house dust mite allergens in Europe: the European Community Respiratory Health Survey II. *J Allergy Clin Immunol* 118: 682–690, 2006. doi:10.1016/j.jaci.2006.04.060.
- Fernández-Caldas E, Puerta L, Caraballo L. Mites and allergy, in history of allergy. 234–242, 2014. doi:10.1159/000358860.
- Li L, Qian J, Zhou Y, Cui Y. Domestic mite-induced allergy: causes, diagnosis, and future prospects. *Int J Immunopathol Pharmacol* 32: 2058738418804095, 2018. doi:10.1177/2058738418804095.
- Deb R, Shakib F, Reid K, Clark H. Major house dust mite allergens Dermatophagoides pteronyssinus 1 and Dermatophagoides farinae 1 degrade and inactivate lung surfactant proteins A and D. *J Biol Chem* 282: 36808–36819, 2007. doi:10.1074/jbc.M702336200.
- Stevenson CS, Birrell MA. Moving towards a new generation of animal models for asthma and COPD with improved clinical relevance. *Pharmacol Ther* 130: 93–105, 2011. doi:10.1016/j.pharmthera.2010.10.008.
- Nials AT, Uddin S. Mouse models of allergic asthma: acute and chronic allergen challenge. *Dis Model Mech* 1: 213–220, 2008. doi:10.1242/dmm.000323.
- Johnson JR, Wiley RE, Fattouh R, Swirski FK, Gajewska BU, Coyle AJ, Gutierrez-Ramos J-C, Ellis R, Inman MD, Jordana M. Continuous exposure to house dust mite elicits chronic airway inflammation and structural remodeling. *Am J Respir Crit Care Med* 169: 378–385, 2004. doi:10.1164/rccm.200308-1094OC.
- Casimir GJ, Lefèvre N, Corazza F, Duchateau J. Sex and inflammation in respiratory diseases: a clinical viewpoint. *Biol Sex Differ* 4: 16, 2013. doi:10.1186/2042-6410-4-16.
- Arnold AP. Four Core Genotypes and XY* mouse models: update on impact on SABV research. *Neurosci Biobehav Rev* 119: 1–8, 2020. doi:10.1016/j.neubiorev.2020.09.021.
- Boissier J, Chlichia K, Digion Y, Ruppel A, Moné H. Preliminary study on sex-related inflammatory reactions in mice infected with *Schistosoma mansoni*. *Parasitol Res* 91: 144–150, 2003. doi:10.1007/s00436-003-0943-1.
- Xia HJ, Zhang GH, Wang RR, Zheng YT. The influence of age and sex on the cell counts of peripheral blood leukocyte subpopulations in Chinese rhesus macaques. *Cell Mol Immunol* 6: 433–440, 2009. doi:10.1038/cmi.2009.55.
- Melgert BN, Oriss TB, Qi Z, Dixon-McCarthy B, Geerlings M, Hylkema MN, Ray A. Macrophages: regulators of sex differences in asthma? *Am J Respir Cell Mol Biol* 42: 595–603, 2010. doi:10.1165/rcmb.2009-0016OC.
- Yovel G, Shakhar K, Ben-Eliyahu S. The effects of sex, menstrual cycle, and oral contraceptives on the number and activity of natural killer cells. *Gynecol Oncol* 81: 254–262, 2001. doi:10.1006/gyno.2001.6153.
- Klein SL, Jedlicka A, Pekosz A. The Xs and Y of immune responses to viral vaccines. *Lancet Infect Dis* 10: 338–349, 2010 [Erratum in *Lancet Infect Dis* 10: 740, 2010]. doi:10.1016/S1473-3099(10)70049-9.
- Cook IF. Sexual dimorphism of humoral immunity with human vaccines. *Vaccine* 26: 3551–3555, 2008. doi:10.1016/j.vaccine.2008.04.054.
- Koçar IH, Yesilova Z, Özata M, Turan M, Sengül A, Özdemir İÇ. The effect of testosterone replacement treatment on immunological features of patients with Klinefelter's syndrome. *Clinical & Experimental Immunology* 121: 448–452, 2001. doi:10.1046/j.1365-2249.2000.01329.x.
- Musabak U, Bolu E, Ozata M, Oktenli C, Sengul A, Inal A, Yesilova Z, Kilicler G, Ozdemir IC, Kocar IH. Gonadotropin treatment restores in vitro interleukin-1beta and tumour necrosis factor- alpha

- production by stimulated peripheral blood mononuclear cells from patients with idiopathic hypogonadotropic hypogonadism. *Clin Exp Immunol* 132: 265–270, 2003. doi:10.1046/j.1365-2249.2003.02141.x.
25. Malkin CJ, Pugh PJ, Jones RD, Kapoor D, Channer KS, Jones TH. The effect of testosterone replacement on endogenous inflammatory cytokines and lipid profiles in hypogonadal men. *J Clin Endocrinol Metab* 89: 3313–3318, 2004. doi:10.1210/jc.2003-031069.
 26. Liva SM, Voskuhl RR. Testosterone acts directly on CD4⁺ T lymphocytes to increase IL-10 production. *J Immunol* 167: 2060–2067, 2001. doi:10.4049/jimmunol.167.4.2060.
 27. Dai R, Phillips RA, Zhang Y, Khan D, Crasta O, Ahmed SA. Suppression of LPS-induced interferon- γ and nitric oxide in splenic lymphocytes by select estrogen-regulated microRNAs: a novel mechanism of immune modulation. *Blood* 112: 4591–4597, 2008. doi:10.1182/blood-2008-04-152488.
 28. Paharkova-Vatchkova V, Maldonado R, Kovats S. Estrogen preferentially promotes the differentiation of CD11c⁺ CD11bintermediate dendritic cells from bone marrow precursors. *J Immunol* 172: 1426–1436, 2004. doi:10.4049/jimmunol.172.3.1426.
 29. Escribese MM, Kraus T, Rhee E, Fernandez-Sesma A, López CB, Moran TM. Estrogen inhibits dendritic cell maturation to RNA viruses. *Blood* 112: 4574–4584, 2008. doi:10.1182/blood-2008-04-148692.
 30. Straub RH. The complex role of estrogens in inflammation. *Endocr Rev* 28: 521–574, 2007. doi:10.1210/er.2007-0001.
 31. Giraud SN, Caron CM, Pham-Dinh D, Kitabgi P, Nicot AB. Estradiol inhibits ongoing autoimmune neuroinflammation and NF κ B-dependent CCL2 expression in reactive astrocytes. *Proc Natl Acad Sci USA* 107: 8416–8421, 2010. doi:10.1073/pnas.0910627107.
 32. Mao G, Wang J, Kang Y, Tai P, Wen J, Zou Q, Li G, Ouyang H, Xia G, Wang B. Progesterone increases systemic and local uterine proportions of CD4⁺ CD25⁺ Treg cells during midterm pregnancy in mice. *Endocrinology* 151: 5477–5488, 2010. doi:10.1210/en.2010-0426.
 33. Jones LA, Kreem S, Shweash M, Paul A, Alexander J, Roberts CW. Differential modulation of TLR3-and TLR4-mediated dendritic cell maturation and function by progesterone. *J Immunol* 185: 4525–4534, 2010. doi:10.4049/jimmunol.0901155.
 34. Butts CL, Bowers E, Horn JC, Shukair SA, Belyavskaya E, Tonelli L, Sternberg EM. Inhibitory effects of progesterone differ in dendritic cells from female and male rodents. *Genet Med* 5: 434–447, 2008. doi:10.1016/j.genm.2008.11.001.
 35. Stamova B, Tian Y, Jickling G, Bushnell C, Zhan X, Liu D, Ander BP, Verro P, Patel V, Pevec WC, Hedayati N, Dawson DL, Jauch EC, Pancioli A, Broderick JP, Sharp FR. The X-chromosome has a different pattern of gene expression in women compared with men with ischemic stroke. *Stroke* 43: 326–334, 2012. doi:10.1161/STROKEAHA.111.629337.
 36. Libert C, Dejager L, Pinheiro I. The X chromosome in immune functions: when a chromosome makes the difference. *Nat Rev Immunol* 10: 594–604, 2010. doi:10.1038/nri2815.
 37. Pisitkun P, Deane JA, Difilippantonio MJ, Tarasenko T, Satterthwaite AB, Bolland S. Autoreactive B cell responses to RNA-related antigens due to TLR7 gene duplication. *Science* 312: 1669–1672, 2006. doi:10.1126/science.1124978.
 38. Fish EN. The X-files in immunity: sex-based differences predispose immune responses. *Nat Rev Immunol* 8: 737–744, 2008. doi:10.1038/nri2394.
 39. Spach KM, Blake M, Bunn JY, McElvany B, Noubade R, Blankenhorn EP, Teuscher C. Cutting edge: the Y chromosome controls the age-dependent experimental allergic encephalomyelitis sexual dimorphism in SJL/J mice. *J Immunol* 182: 1789–1793, 2009. doi:10.4049/jimmunol.0803200.
 40. Dillon SP, Kurien BT, Li S, Bruner GR, Kaufman KM, Harley JB, Gaffney PM, Wallace DJ, Weisman MH, Scofield RH. Sex chromosome aneuploidies among men with systemic lupus erythematosus. *J Autoimmun* 38: J129–J134, 2012. doi:10.1016/j.jaut.2011.10.004.
 41. Arnold AP, Lusis AJ. Understanding the sexome: measuring and reporting sex differences in gene systems. *Endocrinology* 153: 2551–2555, 2012. doi:10.1210/en.2011-2134.
 42. Ekpruke CD, Alford R, Rousselle D, Babayev M, Sharma S, Commodore S, Buechlein A, Rusch DB, Silveyra P. Transcriptomics analysis of allergen-induced inflammatory gene expression in the Four-Core Genotype mouse model. *Physiol Genomics* 56: 235–245, 2024. doi:10.1152/physiolgenomics.00112.2023.
 43. Bracken SJ, Adami AJ, Szczepanek SM, Ehsan M, Natarajan P, Guernsey LA, Shahriari N, Rafti E, Matson AP, Schramm CM, Thrall RS. Long-term exposure to house dust mite leads to the suppression of allergic airway disease despite persistent lung inflammation. *Int Arch Allergy Immunol* 166: 243–258, 2015. doi:10.1159/000381058.
 44. Veress LA, O'Neill HC, Hendry-Hofer TB, Loader JE, Rancourt RC, White CW. Airway obstruction due to bronchial vascular injury after sulfur mustard analog inhalation. *Am J Respir Crit Care Med* 182: 1352–1361, 2010. doi:10.1164/rccm.200910-1618OC.
 45. Monaghan KL, Farris BY, Zheng W, Wan ECK. Characterization of immune cells and proinflammatory mediators in the pulmonary environment. *J Vis Exp* 160: e61359, 2020. doi:10.3791/61359.
 46. Ekpruke CD, Borges-Sosa O, Hassel CA, Rousselle D, Dinwiddie L, Babayev M, Bakare A, Silveyra P. Sex-specific anti-inflammatory effects of a ketogenic diet in a mouse model of allergic airway inflammation. *Int J Mol Sci* 26: 3046, 2025. doi:10.3390/ijms26073046.
 47. Lenth R. emmeans: Estimated Marginal Means, Aka Least-Squares Means. R Package Version. Vienna, Austria: Comprehensive R Archive Network, 2022. <https://cran.r-project.org/package=emmeans>.
 48. Kassambara A. ggpubr: 'Ggplot2' Based Publication Ready Plots. R Package Version. Vienna, Austria: The Comprehensive R Archive Network, 2022. <https://cran.r-project.org/web/packages/ggpubr/index.html>.
 49. Sjoberg DD, Whiting K, Curry M, Lavery JA, Larmarange J. Reproducible summary tables with the gtsummary package. *RJ* 13: 570–580, 2021. doi:10.32614/RJ-2021-053.
 50. Kuznetsova A, Brockhoff PB, Christensen RH. lmerTest package: tests in linear mixed effects models. *J Stat Soft* 82: 1–26, 2017. doi:10.18637/jss.v082.i13.
 51. Wickham H, Averick M, Bryan J, Chang W, McGowan L, François R, Grolemund G, Hayes A, Henry L, Hester J, Kuhn M, Pedersen T, Miller E, Bache S, Müller K, Ooms J, Robinson D, Seidel D, Spinu V, Takahashi K, Vaughan D, Wilke C, Woo K, Yutani H. Welcome to the Tidyverse. *JOSS* 4: 1686, 2019. doi:10.21105/joss.01686.
 52. Mukherjee AB, Zhang Z. Allergic asthma: influence of genetic and environmental factors. *J Biol Chem* 286: 32883–32889, 2011. doi:10.1074/jbc.R110.197046.
 53. Murrison LB, Brandt EB, Myers JB, Hershey GKK. Environmental exposures and mechanisms in allergy and asthma development. *J Clin Invest* 129: 1504–1515, 2019. doi:10.1172/JCI124612.
 54. Wang J, Zhou Y, Zhang H, Hu L, Liu J, Wang L, Wang T, Zhang H, Cong L, Wang Q. Pathogenesis of allergic diseases and implications for therapeutic interventions. *Signal Transduct Target Ther* 8: 138, 2023. doi:10.1038/s41392-023-01344-4.
 55. Schulze J, Voss S, Zissler U, Rose MA, Zielen S, Schubert R. Airway responses and inflammation in subjects with asthma after four days of repeated high-single-dose allergen challenge. *Respir Res* 13: 78, 2012. doi:10.1186/1465-9921-13-78.
 56. Stevens NC, Brown VJ, Domanico MC, Edwards PC, Van Winkle LS, Fiehn O. Alteration of glycosphingolipid metabolism by ozone is associated with exacerbation of allergic asthma characteristics in mice. *Toxicol Sci* 191: 79–89, 2023. doi:10.1093/toxsci/kfac117.
 57. Kabesch M, Tost J. Recent findings in the genetics and epigenetics of asthma and allergy. *Semin Immunopathol* 42: 43–60, 2020. doi:10.1007/s00281-019-00777-w.
 58. Ekpruke CD, Alford R, Rousselle D, Babayev M, Sharma S, Parker E, Davis K, Hemmerich C, Rusch DB, Silveyra P. Sex-specific alterations in the gut and lung microbiome of allergen-induced mice. *Front Allergy* 5: 1451846, 2024. doi:10.3389/falgy.2024.1451846.
 59. Malaviya R, Zhou Z, Raymond H, Wertheimer J, Jones B, Bunting R, Wilkinson P, Madireddy L, Hall L, Ryan M, Rao TS. Repeated exposure of house dust mite induces progressive airway inflammation in mice: Differential roles of CCL17 and IL-13. *Pharmacol Res Perspect* 9: e00770, 2021. doi:10.1002/prp2.770.
 60. Piyadasa H, Altieri A, Basu S, Schwartz J, Halayko AJ, Mookherjee N. Biosignature for airway inflammation in a house dust mite-challenged murine model of allergic asthma. *Biol Open* 5: 112–121, 2016. doi:10.1242/bio.014464.
 61. Ricciardolo FLM, Guida G, Bertolini F, Di Stefano A, Carriero V. Phenotype overlap in the natural history of asthma. *Eur Respir Rev* 32: 220201, 2023. doi:10.1183/16000617.0201-2022.

62. **Hogaboam CM, Blease K, Mehrad B, Steinhauser ML, Standiford TJ, Kunkel SL, Lukacs NW.** Chronic airway hyperreactivity, goblet cell hyperplasia, and peribronchial fibrosis during allergic airway disease induced by *Aspergillus fumigatus*. *Am J Pathol* 156: 723–732, 2000. doi:10.1016/S0002-9440(10)64775-X.
63. **Saito A, Koya T, Aoki A, Naramoto S, Ueno H, Nishiyama Y, Shima K, Kimura Y, Hasegawa T, Watanabe S, Ohshima Y, Suzuki K, Ohashi-Doi K, Kikuchi T.** Mechanism differences in the start time of sublingual immunotherapy in a mouse allergic airway inflammation model. *Sci Rep* 14: 26334, 2024. doi:10.1038/s41598-024-78062-6.
64. **Kim DW, Eun KM, Jin HR, Cho SH, Kim DK.** Prolonged allergen exposure is associated with increased thymic stromal lymphopoietin expression and Th2-skewing in mouse models of chronic rhinosinusitis. *Laryngoscope* 126: E265–E272, 2016. doi:10.1002/lary.26004.
65. **Peng RD, Paigen B, Eggleston PA, Hagberg KA, Krevans M, Curtin-Brosnan J, Benson C, Shreffler WG, Matsui EC.** Both the variability and level of mouse allergen exposure influence the phenotype of the immune response in workers at a mouse facility. *J Allergy Clin Immunol* 128: 390–396.e7, 2011. doi:10.1016/j.jaci.2011.04.050.
66. **Blacquièrè MJ, Hylkema MN, Postma DS, Geerlings M, Timens W, Melgert BN.** Airway inflammation and remodeling in two mouse models of asthma: comparison of males and females. *Int Arch Allergy Immunol* 153: 173–181, 2010. doi:10.1159/000312635.
67. **Mostafa DHD, Hemshekhar M, Piyadasa H, Altieri A, Halayko AJ, Pascoe CD, Mookherjee N.** Characterization of sex-related differences in allergen house dust mite-challenged airway inflammation, in two different strains of mice. *Sci Rep* 12: 20837, 2022. doi:10.1038/s41598-022-25327-7.
68. **Draijer C, Peters-Golden M.** Alveolar macrophages in allergic asthma: the forgotten cell awakes. *Curr Allergy Asthma Rep* 17: 12, 2017. doi:10.1007/s11882-017-0681-6.
69. **Pribul PK, Harker J, Wang B, Wang H, Tregoning JS, Schwarze J, Openshaw PJM.** Alveolar macrophages are a major determinant of early responses to viral lung infection but do not influence subsequent disease development. *J Virol* 82: 4441–4448, 2008. doi:10.1128/JVI.02541-07.
70. **Jacobsen EA, Ochkur SI, Pero RS, Taranova AG, Protheroe CA, Colbert DC, Lee NA, Lee JJ.** Allergic pulmonary inflammation in mice is dependent on eosinophil-induced recruitment of effector T cells. *J Exp Med* 205: 699–710, 2008. doi:10.1084/jem.20071840.
71. **Jacobsen EA, Lee NA, Lee JJ.** Re-defining the unique roles for eosinophils in allergic respiratory inflammation. *Clin Exp Allergy* 44: 1119–1136, 2014. doi:10.1111/cea.12358.
72. **GeurtsvanKessel CH, Lambrecht BN.** Division of labor between dendritic cell subsets of the lung. *Mucosal Immunol* 1: 442–450, 2008. doi:10.1038/mi.2008.39.
73. **Baldaçara RP, Silva I.** Association between asthma and female sex hormones. *Sao Paulo Med J* 135: 4–14, 2017. doi:10.1590/1516-3180.2016.011827016.
74. **Fuentes N, Silveyra P.** Endocrine regulation of lung disease and inflammation. *Exp Biol Med (Maywood)* 243: 1313–1322, 2018. doi:10.1177/1535370218816653.
75. **Cephus JY, Gandhi VD, Shah R, Brooke Davis J, Fuseini H, Yung JA, Zhang J, Kita H, Polosukhin VV, Zhou W, Newcomb DC.** Estrogen receptor- α signaling increases allergen-induced IL-33 release and airway inflammation. *Allergy* 76: 255–268, 2021. doi:10.1111/all.14491.
76. **Keselman A, Fang X, White PB, Heller NM.** Estrogen signaling contributes to sex differences in macrophage polarization during asthma. *J Immunol* 199: 1573–1583, 2017. doi:10.4049/jimmunol.1601975.
77. **Matsubara S, Swasey CH, Loader JE, Dakhama A, Joetham A, Ohnishi H, Balhorn A, Miyahara N, Takeda K, Gelfand EW.** Estrogen determines sex differences in airway responsiveness after allergen exposure. *Am J Respir Cell Mol Biol* 38: 501–508, 2008. doi:10.1165/rcmb.2007-0298OC.